RSC Advances

ROYAL SOCIETY OF CHEMISTRY

www.rsc.org/advances

Fluorofenidone-loaded PLGA microspheres for targeted treatment of paraquat-induced acute lung injury in rats

Authors: Jing Tang[a], Zhenbao Liu[b], Yue Zhang[b], Ling Wang[a], Dai Li[c], Jinsong Ding[b*], Xuehua Jiang[a*]

[a]Key Laboratory of Drug Targeting and Drug Delivery System, West China School of Pharmacy, Sichuan University, No. 17, Section 3, South Renmin Road, Chendu 610041, Sichuan, PR China

[b]School of Pharmaceutical Sciences, Central South University, 172 Tongzipo Road, Changsha 410013, Hunan, PR China

[c]Xiangya Hospital, Central South University, 87 Xiangya Road, Changsha 410008, Hunan, PR China

Corresponding authors:

[*a]Xuehua Jiang

Professor, West China School of Pharmacy

Sichuan University, South Renmin Road,Chendu 610041

Sichuan, PR China

Tel: +86 28 85503024.

E-mail: jxh1013@scu.edu.cn (XH.Jiang).

[*b]Jinsong Ding

Professor, School of Pharmaceutical Sciences

Central South University, 172 Tongzipo Road, Changsha 410013

Hunan, PRChina.

Tel: +86 731 82650250.

E-mail: dingjs0221@163.com (JS.Ding).

Abstract

Lung-targeting fluorofenidone (AKF) loaded PLGA microspheres (AKF-MS) for the treatment of paraquat (PQ)-induced acute lung injury in rats，were constructed by a solvent evaporation method. The microspheres' morphology, size distribution, drug loading ratio, encapsulation efficiency, *in vitro* release characteristics and tissue distributions in rats were systematically studied. Scanning electron microscopy shows the microspheres are spherical and well dispersed. The average particle size is 18.1 μm with 90% of the microspheres being in the range of 7 to 30 μm. The encapsulation efficiency (EE%) and drug loading ratio (DL%) are 80.2 ±2.5% and 8.2 ± 1.9%, respectively. The *in vitro* drug release behavior of AKF-MS follows the Korsmeyer-Peppas model: $Q=11.141 \cdot t^{0.292}$ ($R^2 = 0.9797$). The tissue distribution shows that the drug concentrations in lung tissue for the AKF-MS/18.1 μm suspension is significantly higher than those for the AKF solution and the AKF-MS/3.9 μm, and the drug-targeting index for lung is 6.4 and 4.6-fold higher than that of AKF solution and AKF-MS/3.9 μm, respectively. In addition, AKF-MS/18.1 μm significantly reduced the circulating levels of TNF-α and IL-1β. Histopathological studies confirm that the AKF-MS treatment significantly reduced the edema and neutrophil infiltration, as well as the lung interval damage. Taken together, the results of the present study demonstrated that AKF-MS/18.1 μm improved the treatment efficacy of AKF against PQ-induced acute lung injury, compared to other forms of AKF (AKF solution and AKF-MS/3.9 μm).

Keywords: paraquat· fluorofenidone· acute lung injury· PLGA microspheres· lung-targeting

1. Introduction

Paraquat (1, 1′-dimethyl-4, 4′-bipyridylium dichloride, PQ, **Figure 1a**) [CAS number 1910-42-5], a type of bipyridylium quaternary ammonium herbicide, has been widely used in agriculture owning to its efficiency, especially in developing countries.[1] However, PQ is highly toxic. Accidental exposure to PQ can cause serious poisoning and the mortality rate is between 50% and 90%.[2] The high fatality of PQ is partly due to its inherent toxicity and the lack of effective treatment. Aside from supportive care alone, current treatment of PQ poisoning involves various combinations of immune-modulation (cyclophosphamide, MESNA, methylprednisolone and dexamethasone), anti-oxidant therapy (Vitamin E, Vitamin C, N-acetylcysteine, Salicylic acid and Deferoxamine), haemoperfusion and haemodialysis.[3-5] Nevertheless, the overall mortality remains high even in hospital routinely practising such intensive treatment.

The lung is the main target organ of PQ. Nearly all PQ poisoning cases lead to acute lung injury and, ultimately, acute respiratory distress syndrome.[6] PQ tends to accumulate in the lung tissue, and its pulmonary concentration can be 6-10 times higher than that in plasma.[7] The mechanism for this organ specificity is postulated to be associated with the active polyamine uptake transport systems that concentrate PQ rapidly into the type II epithelial cells of the alveoli.[8] Generally, the mechanism of PQ toxicity involves a redox cyclic reaction, which generates superoxide anions, singlet oxygen and other free radicals, resulting in the depletion of NADPH with the production of oxygen free radicals.[9, 10] The free radicals generated by the oxidation of PQ can interact with membrane lipids leading to genetic overexpression of fibrogenic cytokines.[8] The pathological changes induced by PQ involve fibroblast proliferation and augmented collagen synthesis in the lung.[11] Therefore, the initiation of PQ-induced lung injury is critically linked with pulmonary fibrosis. Accordingly, anti-fibrotic drug is promising for PQ -induced lung injury treatment.

Fluorofenidone (AKF), 5-methyl-1-(3-fluorophenyl)-2-[1H]-pyridone (**Figure 1b**), is a novel but well validated anti-fibrotic drug.[12-15] The mechanism of AKF involves the down regulation of connective tissue growth factor (CTGF) expression induced by transforming growth factor (TGF-β1) and the related signaling pathway.[16] It is also suggested that AKF inhibits the generation of reactive oxygen species (ROS) induced by AngII and mediates the corresponding tissue repair. Meanwhile, it greatly reduces the over expression and activity of NADPH oxidase.[12] Thus, we hypothesized that AKF might be a candidate for the treatment of PQ-induced acute lung injury. Moreover, pyridine agents, such as pirfenidone [PD. 5-methyl-1-phenyl-2(1H)-pyridone], are effective in treating idiopathic interstitial pneumonia, which can prevent and reverse tissue fibrosis in several organs (**Figure 1c**).[17,18] With a similar structure as PD, we estimate that AKF may also possess similar effects in preventing and reversing tissue fibrosis.

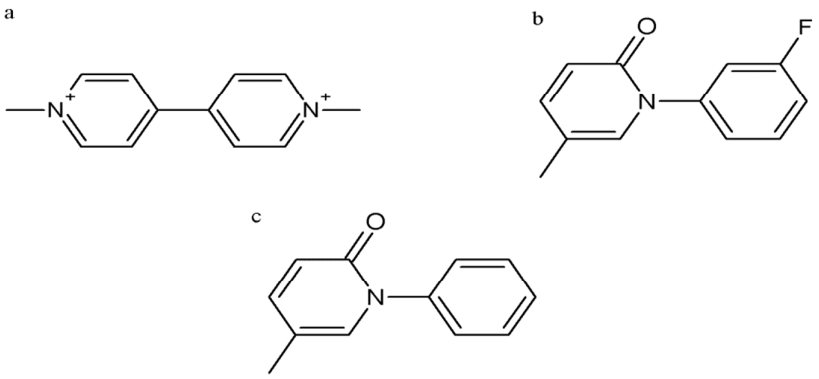

Figure 1 Chemical structure of PQ (a), AKF (b) and PD (c).

However, preliminary studies indicated that AKF distributes widely in the body after oral administration and the concentration in lung is very low. In order to treat PQ-induced acute lung injury, targeted delivery of AKF is important. Microspheres are ideal vehicles to meet this requirement. With diameter ranges from 12 to 44 μm, microspheres are lung-targeting due to

mechanical trapping effect in pulmonary blood vessels.[19, 20] This technique is expected to increase the AKF concentration in lung and, thusly, maximize the efficacy while minimize the potential adverse side effects.

In this work, AKF loaded microspheres (AKF-MS) were prepared and characterized in terms of morphology, particle size and *in vitro* release characteristics. The drug-targeting index (DTI) of AKF-MS was measured to evaluate the potential to be a targeted delivery system for drugs administrated intravenously. The pharmacodynamics study was undertaken to compare the efficacy of AKF-MS with AKF in prevention of lung injury and changing cytokine levels in acutely PQ poisoned rats.

2. Materials and methods

2.1 Materials

AKF (purity＞99%, Lot No. 070704) was synthesized in the School of Pharmaceutical Sciences of Central South University, China. PQ was purchased from Syngenta China Co., Ltd. PLGA (50 : 50, MW = 18 000) was obtained from Jinan Dai Gang Biomaterial Co., Ltd. Polyvinyl alcohol (PVA) was from Sigma Aldrich (MO , USA). Chloral hydrate was from Hecang Chemical Co., LTD (Shanghai, China). TNF-α, IL-1β and NF-κB Elisa Kits were purchased from Neobioscience Technology Co., LTD (China). All other reagents of analytical and chromatographic pure grade were obtained from Sinopharm Chemical Reagent Co., Ltd (Shanghai, China). Double deionized water was purified using a Millipore Simplicity System (Millipore, Bedford, MA).

2.2 Preparation of AKF loaded microspheres (AKF-MS)

The AKF-MS was prepared by the solvent evaporation method and was modified based on a previous study.[21] Briefly, 15 mg of AKF was dispersed in 0.5 mL methylene chloride containing 50 mg PLGA by sonication. The resulting organic phase was added drop-wise to 5 mL with 2% PVA (w/v) solution, and then stirred at 300 rpm for 3 h to allow methylene chloride to

evaporate completely. The microspheres were collected and washed three times with double deionized water, and were dried under vacuum for further use. For AKF-MS/3.9 μm, the primary O/W emulsion was formed via homogenization at 3200 rpm for 5 min before evaporation (EmulsiFlex-C3, Avenstin, Canada).

2.3 Morphological characterization and particle sizing

The surface morphology of AKF microspheres was observed using scanning electron microscope (Quanta 650 FEG, FEI, USA). The lyophilized microspheres were mounted on metal stubs with an adhesive carbon tape, sputter-coated with gold and examined under the microscope. The average particle size and size distribution of the microspheres were measured by PM3089-2002 Micro-plus laser particle size analyzer (Malvern Instruments Ltd., Malvern, UK). For this analysis, the lyophilized microspheres were suspended in double deionized water.

2.4 Drug loading and entrapment efficiency

5 mg of AKF loaded microspheres was dispersed in 10 mL acetonitrile. After 15 min of sonication, the sample was filtered and the concentration of AKF in the filtrate was analyzed by HPLC (LC-2010C Shimadzu, Japan). The drug loading (DL) and encapsulation efficiency (EE) were calculated using the following formulas.

$$DL = \frac{Drug\ loaded}{Drug\ loaded + plymer} \times 100\%$$

$$EE\% = \frac{Actual\ drug\ loading}{theoretical\ drug\ loading} \times 100\%$$

2.5 In vitro drug release studies

Drug release from the microspheres was performed by dialysis method. Briefly, 1 mg of AKF-MS was dispersed in 1 mL double deionized water and then transferred into a dialysis bag (MWCO: 3400). Dialysis was performed in a beaker containing 50 mL dissolution medium (phosphate buffer saline, pH 7.4). The beaker was then placed into a thermostatic shaker at 37 °C and 100

rpm (HZQ-C, Ha'erbin Dongming Medical Instrument Factory, China). 1 mL of the dissolution medium was taken at predetermined time intervals for analysis and an equal volume of fresh buffer was added immediately. The concentration of the released AKF was determined using HPLC. Then, the accumulative release of AKF was calculated as a function of time.

2.6 Tissue distribution

Prior to experiments, 75 SD male rats were divided into 3 groups with 25 in each. All the animals were fasted for 12 h pre-injection, but with free access to water. All animal experiments were conducted in accordance with the Institutional Animal Ethics Committee and Animal Care Guidelines of Central South University governing the use of experimental animals. Firstly, each animal was intraperitoneal (i.p.) injected with PQ at a dose of 30 mg/kg to simulate the pathological state. After 30 min, each group of rats were injected with AKF-MS/3.9 μm, AKF-MS/18.1 μm or AKF solution (dissolved in physiological saline) with the dosage of 30 mg/kg through tail veins, respectively. At 0.5, 6, 12, 24 and 48 h, 5 rats per group were injected with chloral hydrate (400 mg/kg, i.p.) and sacrificed by cervical dislocation. Soon after the sacrifice, the drug in blood, heart, lung, liver, kidney and spleen were extracted. The concentrations of the drug in different tissues were determined by HPLC. For sample preparation, the organs were homogenized, extracted with 1.0 mL acetonitrile using ultrasonic for 1 h, centrifuged at 12,000 rpm for 5 min, and filtered through 0.22 μm filter (Millipore).

2.7 ELISA assay and histopathological studies

150 SD rats were equally divided into 5 groups. The control group received normal saline. Three experimental groups were injected with AKF-MS/3.9 μm, AKF-MS/18.1 μm and AKF solution, respectively, with a dosage of 30 mg/kg after administration of PQ. For the positive control group, only PQ was injected. For each group, five rats were sacrificed at 0, 0.5, 6, 12, 24 and 48 h after injection. Then, the lungs were dissected and washed with saline. The lung tissues were fixed in 10% formaldehyde, embedded in

paraffin, and stained with hematoxylin-eosin (HE). All lung samples were examined using a light microscope. The levels of TNF-α, IL-1β and NF-κB in the lung tissues were determined using commercially available ELISA kits. The levels of TNF-α, IL-1β and NF-κB were calculated with reference to standard curves of purified recombinant TNF-α, IL-1β or NF-κB at various dilutions.

2.8 Statistical analysis

Results expressed as mean ± SD were analyzed using student's t-test or one-way ANOVA by SPSS 19.0. *P*-values < 0.05 were considered as statistically significant.

3. Results and discussion

3.1 Preparation of the PLGA microspheres

The AKF loaded PLGA microspheres were prepared by solvent evaporation method. The entrapment efficiency (EE) % and particle size are the two key physicochemical properties of microspheres. The EE (%) is important for assessing the drug loading (DL) capacity, and thus increasing EE (%) can reduce the loss of drug and help to extend the duration and dosage of treatment. The optimum formulation was selected based on orthogonal experiment design. The influence of the initial O/W ratio (1 : 10, 1 : 15, and 1 : 20), drug/polymer ratio (0.5 : 1, 1 : 5, and 1.5 : 5) and shearing velocity (800, 1600, and 3200 rpm) were evaluated, and particle size (μm), EE(%) and DL(%) were chosen as the optimizing indexes. Only O/W ratio has a significant influence on the properties of microspheres. Since EE (%) and DL (%) tend to decrease at high O/W ratio, O/W (1: 10) was chosen for further study. Finally, the optimized formulation was achieved with 10% PLGA concentration (w/v), 2% PVA concentration (w/v) and 1:10 O/W ratio (v/v), respectively. The average DL (%) and EE (%) at the optimal experimental condition were (8.2 ± 1.9)% and (80.2 ± 2.5)%, respectively.

3.2. Particle morphology and size distribution of the PLGA microspheres

Particle size distribution is an important particle property since it controls the tissue location of the microspheres after their intra-artery infusion. In addition, the size of microspheres affects the product's potential to become an injection and the drug release rate. It has been reported that microspheres with the size ranges from 12 to 44 μm have a notable lung-targeting efficacy.[22, 23] The surface morphology of AKF loaded PLGA microspheres observed by the scanning electron microscopy (SEM) is shown in **Figure 2A** and **B**, which revealed that the microspheres were spherical in shape with a smooth surface. As a control, a smaller size of AKF-MS was also prepared (**Figure 2A**), and the mean diameter was 3.9 ± 1.6 μm from five batches. More than 90% of the microspheres fell within the size range of 7 to 30 μm, and the mean diameter of the microspheres was 18.1± 1.5 μm (**Figure 2B**).

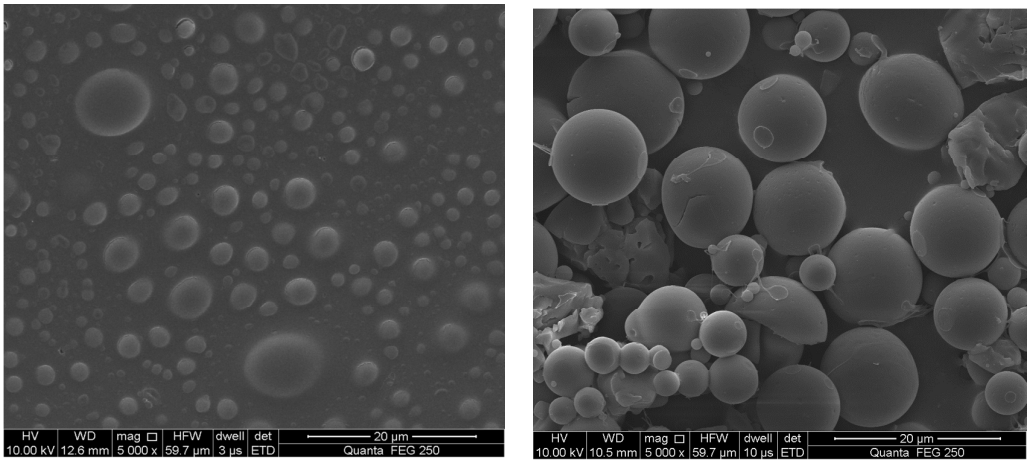

(A) (B)

Figure 2 SEM images of (A) AKF-MS/3.9 μm and (B) AKF-MS/18.1 μm

3.3 In vitro release profile

In vitro release behavior of AKF-MS was performed using the dialysis method. **Figure 3** shows the AKF release curves from AKF-MS and free AKF solution. The free AKF solution showed a burst release with approximate 90% of AKF released within 1 h. On the other hand, the AKF released from AKF-MS presented a two-stage character，i.e. a fast drug release stage was observed in the first 4 h and a subsequent sustained release stage was

monitored over 180 h. The results indicated that the AKF-MS had a well-sustained release capability which is typical for PLGA based drug delivery systems. The data obtained from in vitro release studies fitted various kinetic equations (For examples, zero-order, first-order, Higuchi model, Korsmeyer's Peppas and Hixson-Crowell model).[24-26] The correlation coefficient value, R^2, was taken into account to determine the most suitable model (**Table 1**), and the Korsmeyer-Peppas model appeared to be the one with $R^2 = 0.9797$, suggesting diffusion dominant. The initial "burst" release of AFK from AKF-MS was probably caused by drug releasing from the particle surface facilitated by the swelling of microspheres. AKF-MS/3.9 μm demonstrated a slight faster drug release rate compared to that of 18.1 μm ones during the first 72 h, which might be explained by the relatively larger particle surface area. However, the overall release pattern was quite similar for the two kinds of microspheres ($P< 0.05$), which can be used as ideal comparison for the subsequent study.

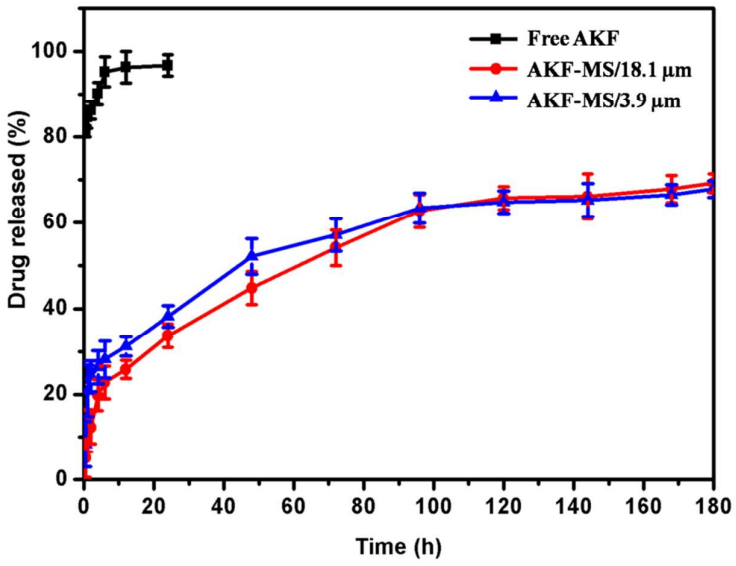

Figure 3 *In vitro* release profiles of free AKF, AKF-MS/18.1 μm and AKF-MS/3.9 μm (n=3)

Table 1. Correlation coefficient values from different model simulation of *in vitro* AKF-MS release data

Zero-order	First-order	Higuchi model	Korsmeyer-Peppas model	Hixson-Crowell model
$Q=0.504 \cdot t$	$Q=100 \cdot [1-Exp(-0.01 \cdot t)]$	$Q=6.039 \cdot t^{0.5}$	$Q=11.141 \cdot t^{0.292}$	$Q=100 \cdot [1-(1-0.003 \cdot t)^3]$
$R^2=0.5462$	$R^2=0.8110$	$R^2=0.9372$	$R^2=0.9797$	$R^2=0.7461$

3.4 Tissue distributions of PLGA microspheres

Lung-targeting effect of AKF-MS was evaluated by drug concentrations in different tissues using HPLC after administration of AKF-MS or AKF intravenously (30 mg/kg). As shown in **Figure 4A**, high drug concentrations were observed in all tissues at 30 min after free drug administration. After that, the drug was cleared and did not selectively accumulate in the lung. It was reasonable since the drug was carried by the blood flow and distributed to all the organs. Without a sustained release mechanism, free AKF was quickly cleared from the body, mainly through urinary elimination. As to AKF-MS/3.9 μm, tissue distribution was quite different (**Figure 4C**), with highest concentrations in liver, spleen, and lung. These results revealed the importance of controlling drug delivery particle size distribution and selecting the size appropriate for avoiding phagocytosis.[27] The uptake of microspheres by human blood neutrophils and leukocytes decreased with increasing particle size in the range of 0.5-8 μm.[28] In all these organs, the drug concentration dropped by roughly half after 6 h and, the concentration dropped to the background level after 1 day. Therefore, the microspheres possessed targeted drug delivery function to some extent.

Very interestingly, when the AKF-MS/18.1 μm microspheres were administrated, the lung displayed the highest drug concentration (**Figure 4B**, the scale of y-axis is different). At the 30 min time point, it was 6.3 times higher than the free AKF injection and 5 times higher than the AKF-MS/3.9 μm. The drug concentration in lung as a function of time was quantified as

shown in **Figure 4D**, clearly indicating that the drug concentrations of AKF-MS/18.1 μm group in lung were significantly higher than those in AKF-MS/3.9 μm and free AKF injection at any subsequently time points.

More importantly, since most of the drug was accumulated in the lungs for AKF-MS/18.1 μm group, very little drug was found in any other tissues. For example, drug concentration in lung was 31.9 times higher than that in plasma (30 min). Compared with the drug targeting index of AKF-MS/18.1 μm in lung was 4.6 and 6.4 times higher than that of AKF-MS/3.9 μm and free AKF, respectively.

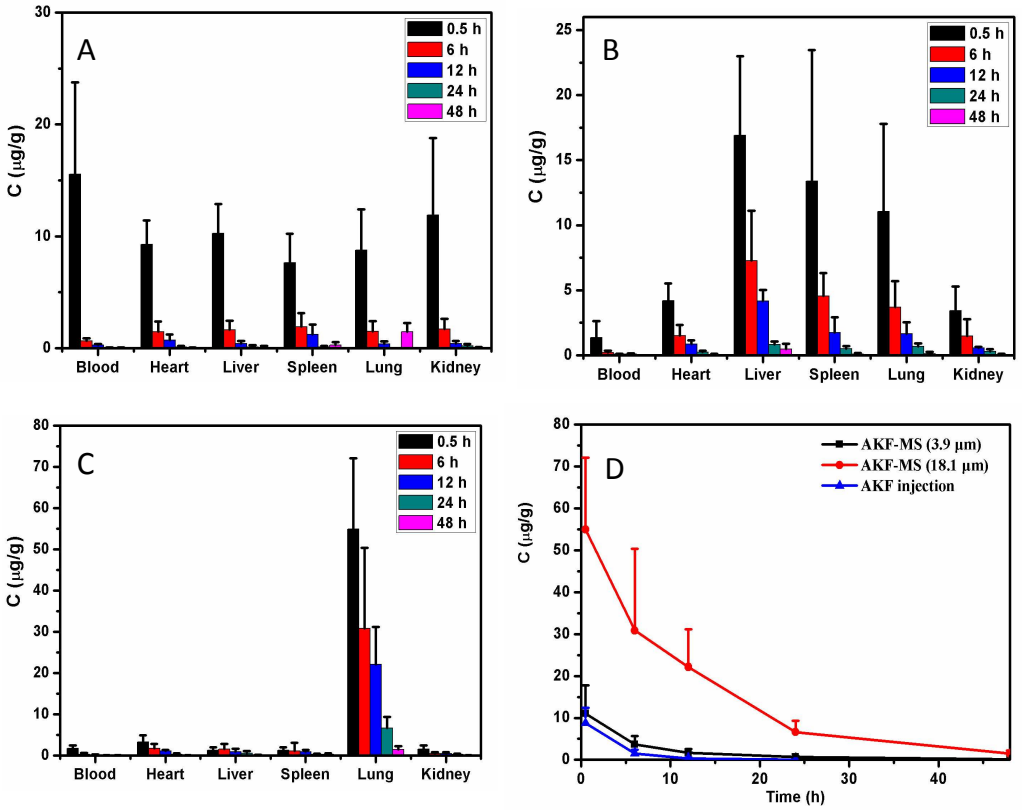

Figure 4 The concentration of AKF in blood, heart, liver, spleen, lung and kidney at 0.5, 6, 12, 24, and 48 h after intravenous administration of AKF injection (30 mg/kg) (A), AKF-MS/3.9 μm (B) and AKF-MS/18.1 μm (C) in rats, and (D) the concentration of AKF in lung of rats with AKF-MS/18.1 μm, AKF–MS/3.9 μm and AKF injection at different time points (Mean ± SD, n=5)

3.5 AKF inhibited PQ-stimulated TNF-α, IL-1β and NF-κB release

PQ causes multiple organ dysfunction syndrome, and mainly acute lung injury. Acute lung injury is characterized by acute lung inflammation involving the local recruitment and activation of polymorphonuclear neutrophils and the release of proinflammatory mediators, proteases, reactive oxygen and nitrogen species.[29,30] Eventually, these processes can cause alveolar-capillary damage with high permeability pulmonary edema and alteration of lung mechanics, resulting in severe gas exchange abnormalities.[31] As the major endotoxin in gram-negative infection, lipopolysaccharide can stimulate the expression of a variety of proinflammatory mediators, including tumor necrosis factor-α (TNF-α), and interleukin 1β (IL-1β).[32] All of them can lead to orchestrate inflammation and tissue damage. The pleiotropic transcription factor nuclear factor-kappa B (NF-κB) plays a crucial role in regulating the expression of cytokines, chemokines, adhesion molecules, and other mediators.[33] So, the protective effect of AKF-MS for acute lung injury was evaluated by these three critical inflammatory factors.

To investigate whether AKF-MS can reduce the release of proinflammatory cytokines, rats were stimulated with PQ in the presence or absence of AKF for specific time. Different formulations of AKF (30mg/kg) were administered i.v. after PQ injection, and the concentrations of TNF-α, IL-1β and NF-κB release were assayed by ELISA kits. As shown in **Figure 5**, levels of the three inflammatory factors in lung were significantly higher than those in the control group, indicating that PQ stimulated the release of proinflammatory cytokines. For the AKF-MS/18.1 μm group, the decreased amounts of TNF-α and IL-1β were in a time-dependent manner (**Figure 5**), indicating that the protective role of AKF-MS in acute lung injury, at least partially, related to the inhibition of the release of the proinflammatory cytokines.

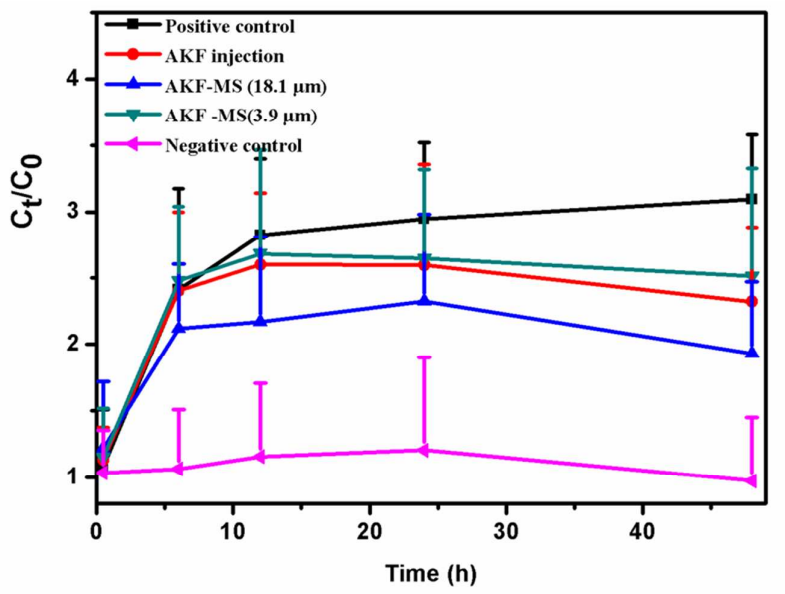

342

343 (A)

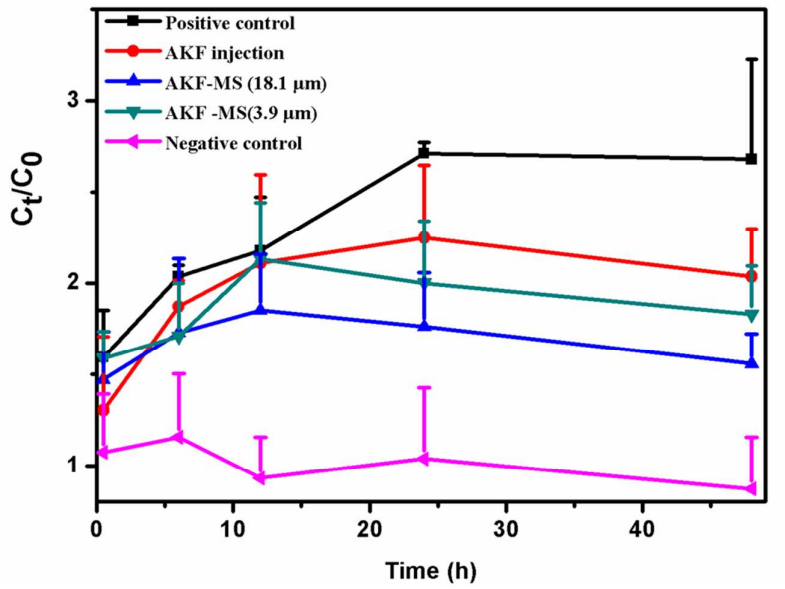

344

345 (B)

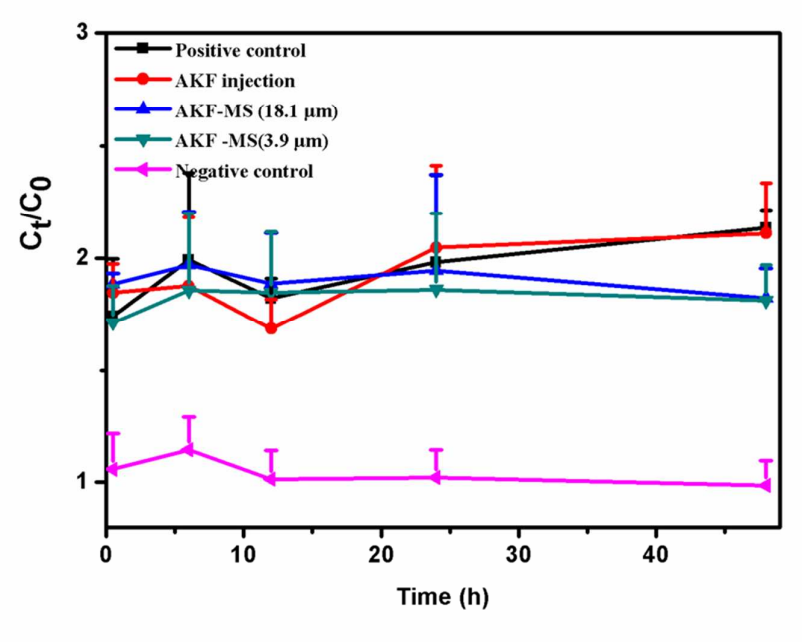

(C)

Figure 5 Cytokines relative concentration versus time of TNF-α (A), IL-1β (B) and NF-κB (C) (Mean ± SD, n=5). C_t represents the measured value of concentration at time t, and C_0 represents the measured value of concentration before drug injection

3.6 Histopathological examination

Photomicrographs of the lung sections after 48 h treatment with AKF-MS are shown in **Figure 6**. In the control group (administrated with normal saline), the alveolar structure was complete, alveolar cavity did not bleed, and there was no neutrophil infiltration (**Figure 6A**).The PQ group displayed significant lung interval damage, alveolar cavity bleeding, and edema and neutrophil infiltration (**Figure 6B**).The free AKF group was characterized by a low level of infiltration of inflammatory cells in the lung interstitium (**Figure 6C**). The lung tissue of the blank microspheres group was similar to that of the PQ group, suggesting that blank microsphere had no therapeutic effect on acute lung injury, while no direct toxicity was found on lung (**Figure 6D**). Compared to the PQ group, pulmonary hemorrhage, interstitial edema, and

infiltration of inflammatory cells were ameliorated to some degree in the lungs of PQ+AKF-MS groups (**Figure 6E, F**). Especially in PQ+AKF-MS/18.1 μm group, the damage was further improved compared to that of the PQ+AKF-MS/3.9 μm group, and less inflammatory cells infiltration was found in the interstitial lung and alveoli, interstitial edema and alveolar hemorrhage were ameliorated. Based on these observations, it could be concluded the microsphere formulation was efficient as a passive targeted drug delivery system to the lung.

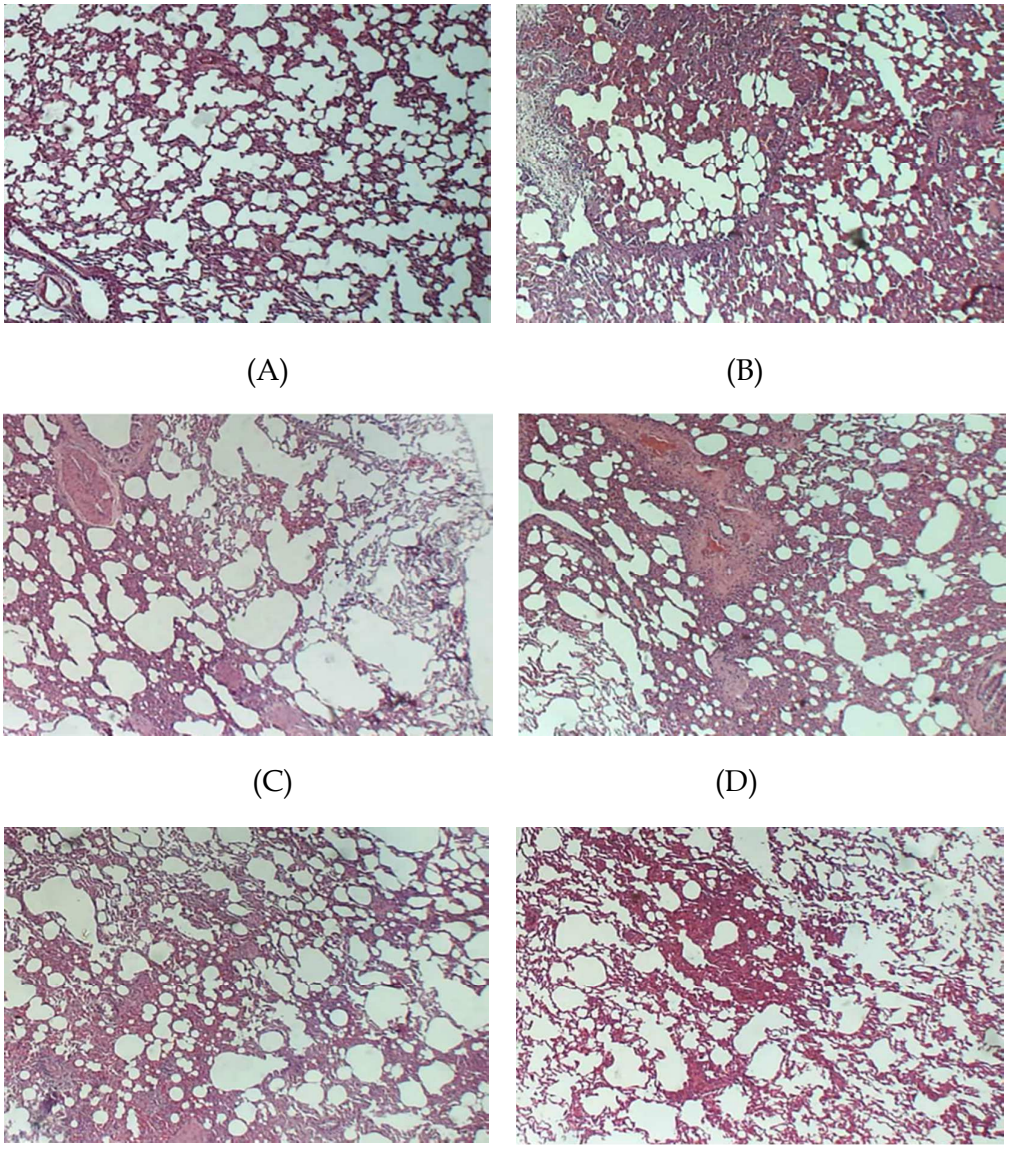

Figure 6 Histological examination of the effects of AKF-MS on PQ-induced

acute lung injury in rats. Free AKF or AKF-MS (equivalent to 30 mg/kg) were intravenously administered to PQ-treated rats. Histological examination was performed by HE staining on the right lung of each rat after PQ administration for 48 h (A–F, ×100). Saline (A), PQ (B), free AKF (C), blank microspheres (D), AKF-MS/3.9 μm (E), and AKF-MS/18.1 μm (F) treated groups.

4. Conclusion

In the present study, AKF-MS/18.1 μm microspheres with high DL (%) and EE (%) were successfully prepared by a solvent evaporation method. *In vitro* release test showed that AKF-MS/18.1 μm exhibited a sustained release characteristic compared with the free drug. AKF-MS/18.1 μm was preferentially located in the lung tissue and was retained for 48 h after intravenous administration. Compared with the AKF solution and AKF-MS/3.9 μm, the drug concentration and the accumulated time of AKF-MS/18.1 μm in the lung tissue were obviously increased while those in non-targeted organs such as heart, kidney, brain, and plasma were effectively reduced. Based on these results, it can be concluded that AKF-MS/18.1 μm can be a promising carrier to deliver AKF to the lung to enhance its therapeutic effects for the treatment of PQ-induced acute lung injury.

Declaration of Interest

The authors declare no conflicts of interest. The authors alone are responsible for the content and writing of this article.

Acknowledgment

This work was supported by grants from National Science and Technology Major Project-The substantial drug discovery initiative (NO. 2009ZX09102-011) and Natural Science Foundation of China (81200047）.

References

1.Wesseling, C., van Wendel de Joode, B., Ruepert, C., Leon, C., Monge, P., Hermosillo, H., Partanen, T. J. *Int J Occup Environ Health*, 2001, **7**, 275-286.

2.Tian, Z. G., Ji, Y., Yan, W. J., Xu, C. Y., Kong, Q. Y., Han, F., Zhao, Y., Pang, Q. F. *Int Immunopharmaco*, 2013, **17**, 309-13.

3.Yeh, S. T., Guo, H. R., Su, Y. S., Lin, H. J., Hou, C. C., Chen, H. M., Chang, M. C., Wang, Y. J. *Toxicology*, 2006, **223**, 181-90.

4.Suntres, Z. E. *Toxicology*, 2002, **180**, 65-77.

5.Gawarammana IB, Buckley NA. Br J Clin Pharmacol 2011,72,745-57.

6.Xu, L., Xu, J., Wang, Z. *Drug Chem Toxicol*, 2014, **37**, 130-4.

7.Dinis-Oliveira, R. J., Duarte, J. A., Sanchez-Navarro, A., Remiao, F., Bastos, M. L., Carvalho, F. *Crit Rev Toxicol*, 2008, **38**, 13-71.

8.Mainwaring, G., Lim, F. L., Antrobus, K., Swain, C., Clapp, M., Kimber, I., Orphanides, G., Moggs, J. G. *Toxicology*, 2006, **225**, 157-72.

9.Dinis-Oliveira, R. J., Sarmento, A., Reis, P., Amaro, A., Remiao, F., Bastos, M. L., Carvalho, F. *Pediatr Emerg Care*, 2006, **22**, 537-40.

10.Dinis-Oliveira, R. J., De Jesus Valle, M. J., Bastos, M. L., Carvalho, F., Sanchez Navarro, A. *Xenobiotica*, 2006, **36**, 724-37.

11.Kim, H. R., Park, B. K., Oh, Y. M., Lee, Y. S., Lee, D. S., Kim, H. K., Kim, J. Y., Shim, T. S., Lee, S. D. *Lung*, 2006, **184**, 287-95.

12.Peng, Z. Z., Hu, G. Y., Shen, H., Wang, L., Ning, W. B., Xie, Y. Y., Wang, N. S., Li, B. X., Tang, Y. T.; Tao, L. J. *Nephrology (Carlton)*, 2009, **14**, 565-72.

13.Tao, L. J., Zhang, J., Hu, G. Y. *Zhong Nan Da Xue Xue Bao Yi Xue Ban*, 2004, **29**, 139-41.

14. Liu, J., Song, C., Xiao, Q., Hu, G., Tao, L., Meng, J.*Shock*, 2014, Publish Ahead of Print. DOI: 10.1097/SHK.0000000000000273.

15. Meng, J., Zou, Y., Hu, C., Zhu, Y., Peng, Z., Hu, G., Wang, Z., Tao, L.*Shock*, 2012, **38**, 567-73.

16.Wang, L., Hu, G. Y., Shen, H., Peng, Z. Z., Ning, W. B., Tao, L. J. *Pharmazie*, 2009, **64**, 680-4.

17. Yamazaki T, Yamashita N, Izumi Y, Nakamura Y, Shiota M, Hanatani A, Shimada K, Muro T, Iwao H, Yoshiyama M. *Hypertens Res*, 2011,**35**, 34-40.

18.Lee KW, Everett TH th, Rahmutula D, Guerra JM, Wilson E, Ding C, Olgin JE. *Circulation*, 2006, 114, 1703-1712.

19.Lu, B., Zhang, J., Yang, H. *Int J Pharm*, 2003, **265**, 1-11.

20 Selek, H., Sahin, S., Kas, H. S., Hincal, A. A., Ponchel, G., Ercan, M. T., Sargon, M. *Drug Dev Ind Pharm*, 2007, **33**, 147-154.

21.Huo, D., Deng, S., Li, L., Ji, J. *Int J Pharm*, 2005, **289**, 63-7.

22.Harsha, S., R, C., Rani, S. *Int J Pharm*, 2009, **380**, 127-32.

23.Hao, Z., Qu, B., Wang, Y., Tang, S., Wang, G., Qiu, M., Zhang, R., Liu, Y., Xiao, X. *Drug Dev Ind Pharm*, 2011, **37**, 1422-8.

24.Stulzer, H. K., Segatto Silva, M. A., Fernandes, D., Assreuy, J. *Drug Deliv*, 2008, **15**, 11-18.

25.Harsha, S., Attimard, M., Khan, T. A., Nair, A. B., Aldhubiab, B. E., Sangi, S., Shariff, A. *J Microencapsul*, 2013, **30**, 257-264.

26.Harsha, N. S., Rani, R. H. *Arch Pharm Res*, 2006, **29**, 598-604.

27. Champion JA.,Walker A., Mitragotri S. *Pharm Res*, 2008, **25**, 1815-21.

28. Simon SI., Schmid-Schönbein GW. *Biophys J*, 1988, **53**, 163-73.

29.Wright, R. M., Ginger, L. A., Kosila, N., Elkins, N. D., Essary, B., McManaman, J. L., Repine, J. E. *Am J Respir Cell Mol Biol*, 2004, **30**, 479-490.
30.Shinbori, T., Walczak, H., Krammer, P. H. *Eur J Immunol*, 2004, **34**, 1762-1770.
31.Liu, D., Zeng, B. X., Shang, Y. *Physiol Res*, 2006, **55**, 291.
32.Liu, D., Zeng, B.-X., Zhang, S.-H., Wang, Y.-L., Zeng, L., Geng, Z.-L., Zhang, S.-F. *Crit Care Med*, 2005, **33**, 2309-2316.
33.Ali, S., Mann, D. A. *Cell Biochem Funct*, 2004, **22**, 67-79.